A BAYESIAN MODELING APPROACH FOR DETERMINING PRODUCTIVITY REGIMES AND THEIR CHARACTERISTICS

S.B. MUNCH[1] and A. KOTTAS[2]

[1]*Marine Science Research Center, Stony Brook University, Stony Brook, NY 11794, USA*

[2]*Department of Applied Mathematics and Statistics, University of California, Santa Cruz, CA 95064, USA*

Abstract. Oscillations in the environment result in substantial alterations to population dynamics as evidenced by time series of abundance and recruitment. Depending on the reference timescale, these oscillations are referred to as regime shifts. Regime shifts may occur on very short time scales and are often undetected for several years. Consequently, tools that allow the estimation of regime-specific population dynamic parameters may be of great value. Using a hidden Markov model to describe the unobserved regime state, we develop methods to infer regime-specific parameters for a commonly used model of density dependent recruitment in addition to identifying the unobserved regime state. We apply the method to recruitment data for Japanese sardine.

Key words: density dependence; hidden Markov model; Japanese sardine; regime shift; stock-recruitment.

INTRODUCTION

One of the fundamental relationships in ecology is the production of offspring as a function of the number of mature individuals. A common way of writing this relationship is $R(S) = aSf(S)$, where R is the number of offspring, S is the number of mature individuals, a is the maximum per capita reproduction (i.e., which occurs in the absence of density dependent factors) and $f(S)$ is a function characterizing the density

dependence of reproduction or juvenile survival. Common measures for S include total egg production, biomass of spawning individuals, or counts of mature indiivudals. In general, we expect that $f(S)$ is close to one when S is small and that $f(S)$ approaches zero as S becomes very large.

A variety of ecological factors are subsumed into the parameters of the reproductive relationship. Both top-down (roughly, predation) and bottom-up (roughly, food) factors affect the production of individuals and it is possible to develop a framework in which these factors are integrated (e.g., Munch et. al. 2005a). However, these biotic factors also depend upon the abiotic environment, so that physical variables are also components in the parameters of the reproductive relationship. Kjesbu et. al. (1998) found a tight correlation between fecundity and both temperature and prey availability. Rates of somatic growth are strongly influenced by temperature and prey availability (Elliot 1994) and combined these effects lead to environmentally induced fluctuations in density dependence (Jacobson and MacCall 1995, Sugimoto et. al. 2001).

Importantly, it is possible for ecosystems to exist in more than one state and that sometimes very rapid changes may occur between the different states of the ecosystem (e.g., Scheffer et. al. 2001, Scheffer and Carpenter 2003, Folke et. al. 2004). Environmental regimes are typically thought of as ecological states that persist over prolonged periods of time. However, precisely how long a state must persist to be considered a regime depends on the context. Regime shifts may require only a few years or several

centuries (Scheffer et. al. 2001) depending upon the reference time scale (e.g., ecological vs geological/evolutionary). In what follows, we refer to different environmental states as regimes, the transition between one state and another as a regime shift, and the productivity of a population in a particular regime as a recruitment regime.

Because our ability to observe the state of ecosystems is imperfect at best, we may not be able to recognize a shift in the state immediately or even directly. However, organisms – through the fundamental process of reproduction with environmental state built into the reproductive parameters – may provide a signal.

For instance, in steelhead trout (*Oncorhynchus mykiss*), juvenile survival varies with environmental state (Welch et. al. 2000) and decadal scale variations in several recruitment time series correspond with shifts in physical variables (e.g., McFarlane et. al. 2000, Daskalov 2003). Moreover, production of sablefish, sardine, English sole, Pacific cod, North Sea plaice, and several salmonids all show pronounced decadal scale fluctuations (McFarlane et. al. 2000, MacCall 2002, Kell and Bromley 2004). Hare and Mantua (2000) review a large number of physical and biological time series and suggest that regime shifts may be more easily recognizable in recruitment indices than in the environmental variables themselves. For example, although the physical data do not unambiguously point to a regime shift in 1986, one is clearly visible in aggregated recruitment patterns of some Pacific groundfishes (Meuter et al. 2007). Similar observations led Tian et al. (2004) to suggest the use of saury as a bioindicator

of regime shifts. We operationalize this idea by constructing a statistical framework in which we infer the regime state and production functions from observed patterns in recruitment.

The simplest case is one in which the environment may exist in two states that are described by a Markov process. Such a case was investigated by Slatkin (1978), who determined those characteristics of environmental fluctuation (via a first order Markov process) and population growth that allow the existence of a stationary distribution of population sizes, concluding that such stationary distributions can exist only when the correlation time of the environmental changes and the response time of the population are comparable. Nisbet and Bence (1989) developed a model for the productivity of giant kelp (*Macrosystis* spp.) in which there are Markovian transitions between two environments. In one environment they assumed recruitment is simply impossible, and in the other environment recruitment is possible, but still stochastic depending upon a variety of possible other states. Our work extends their model to the case where there are two environmental states in which reproduction is possible: one in which reproduction is on average low and one in which reproduction is on average high. In both regimes, reproductive success is density dependent, though the way in which density influences reproduction may differ in each state.

If there is considerable variance around the average reproduction under a given regime and one cannot measure the state of the environment directly, then the prob-

lem becomes that of making inference about the state of the environment and the characteristics of reproduction simultaneously. Here, we propose a new method for fitting regime-specific models for density dependent juvenile survival and simultaneously estimating the regime state. Since the underlying process determining the state of the environment is hidden, we use a Hidden Markov model as the basis of our statistical framework. Hidden Markov Models (HMMs) have played a key role in the revolution in bioinformatics (e.g., Liu et. al. 1999), and are just now becoming used in ecology. Tucker and Anand (2004) argue for the general utility of HMMs in ecology and review their use in a restoration context. Scott (2002) provides a review on Bayesian methods for HMMs. The modeling approach that we adopt here is alternatively referred to as a HMM, Markov-dependent mixture model or Markov switching regression model.

We assume that there are two environmental regimes characterized by distinct productivities (Wada and Jacobson 1998, Hare and Mantua 2000) and that the process governing the regime state is a two-state Markov chain. We employ a Bayesian approach to infer the parameters of the Markov process and regime-specific production functions. This approach allows incorporation of prior information regarding both the regime shifts and the regime-specific density dependence models, and yields full and exact inference for the model parameters.

In the next section, we introduce the methodology, which involves a Markov model for the state of the environment and a Ricker model (Ricker 1954) for $aSf(S)$. We

describe how the modeling framework can be used to estimate the long-term and short-term recruitment distributions. To facilitate use of this approach in situations where the existence of multiple regimes is uncertain, we develop estimates of posterior probabilities corresponding to the one and two-regime models. Details of these calculations are defered, for sake of readability, to Appendices A–C. We then illustrate the methodology with data for Japanese sardine. We conclude with a discussion of our results and comparison of the approach with previous ones.

METHODS

The modeling approach

If the regime states for each year were known, the problem would be straightforward; we could divide the data into regime-specific subsets and fit separate recruitment models to each using standard statistical tools. However, the regime state may be difficult to identify, may shift over a short period of time and may not be adequately characterized for several years following a shift. As a consequence, we require a method that allows us to make inferences regarding the regime state as well as the regime-specific model parameters. Our modeling approach combines a Markov model for unobserved environmental regimes with regime-specific recruitment likelihoods. Within each regime, we assume that recruitment follows a Ricker model with multiplicative log-normal errors. Inference for the model involves assigning priors to the transition probabilities

and recruitment parameters and updating these based on the observed time series. In the next few paragraphs we present a more formal description of the model and then apply it to data for Japanese sardine.

The regime state in year t (denoted by r_t) takes on one of two values (here, 1 or 2) with some probability that depends on the regime state in year $t-1$. That is,

$$\Pr(r_t = i \mid r_{t-1} = j) = q_{ij}, \quad i, j = 1, 2 \tag{1}$$

where the q_{ij} are the probabilities of transitions into regime i from regime j. In the Bayesian context, these transition probabilities themselves require a prior probability model. We use independent Beta distributions for the probabilities of remaining in each regime, i.e., for the q_{jj}, $j = 1, 2$.

For each regime-specific model of juvenile survival, we use the standard Ricker model (Ricker 1954). More general specifications are also feasible as discussed at the end of this section. Specifically, the number of surviving juveniles, hereafter referred to as recruitment (R), is given by

$$R_j(S) = a_j S \exp(-b_j S), \quad j = 1, 2 \tag{2}$$

where S is the total egg prodcution or initial number of individuals in a cohort and the subscript indicates parameters for recruitment under regime j. We assume that errors around the recruitment relationship in Eq. 2 are multiplicative and log-normal. To facilitate model fitting, we consider the transformed variable, $y = \log(R/S)$, resulting

in the log-transformed, re-parameterized recruitment model,

$$y = \alpha_j - \beta_j S, \quad j = 1, 2 \tag{3}$$

where $\alpha_j = \log a_j$ and $\beta_j = b_j$. The errors around the transformed recruitment function in Eq. 3 are additive normal with mean zero and variance V_j. Note that both the recruitment parameters, α_j and β_j, as well as the variance parameter V_j depend on the regime state $j = 1, 2$.

To simplify notation, we gather the regime-specific model parameters into a vector $\boldsymbol{\theta} = (\boldsymbol{\theta}_1, \boldsymbol{\theta}_2)$ with $\boldsymbol{\theta}_j = (\alpha_j, \beta_j)$, $j = 1, 2$, the regime-specific error variances (on the log-scale) into $\boldsymbol{V} = (V_1, V_2)$, and the transition probabilities into a vector $\boldsymbol{Q}$. Moreover, we denote the regime-specific recruitment functions by $F(S; \boldsymbol{\theta}_j) = \alpha_j - \beta_j S$, $j = 1, 2$. The fully specified model is thus given by

$$\begin{aligned} y_t \mid r_t = j, \boldsymbol{\theta}, \boldsymbol{V} &\overset{ind}{\sim} N(y_t \mid F(S_t; \boldsymbol{\theta}_j), V_j), \;\; t = 1, ..., T \\ \{r_1, ..., r_T\} \mid \boldsymbol{Q} &\sim \textstyle\prod_{t=2}^{T} \Pr(r_t \mid r_{t-1}, \boldsymbol{Q}) \\ \boldsymbol{Q}, \boldsymbol{\theta}, \boldsymbol{V} &\sim p(\boldsymbol{Q}) p(\boldsymbol{\theta}) p(\boldsymbol{V}). \end{aligned} \tag{4}$$

Here, $p(\boldsymbol{Q})$, $p(\boldsymbol{\theta})$ and $p(\boldsymbol{V})$ are the prior densities for $\boldsymbol{Q}$, $\boldsymbol{\theta}$ and $\boldsymbol{V}$, T is the final year in which recruitment was observed, and $N(y \mid F(S; \boldsymbol{\theta}_j), V_j)$ denotes a normal density for y with mean $F(S; \boldsymbol{\theta}_j)$ and variance V_j. The transition probabilities $\Pr(r_t \mid r_{t-1}, \boldsymbol{Q})$ are given in Eq. 1. Since the regime designation is abritrary, we set $r_1 = 1$ without loss of generality.

As mentioned above, the prior for $\boldsymbol{Q}$ is built from independent Beta distributions

for the q_{jj}, $j = 1, 2$. We take independent inverse gamma priors for the V_j, $j = 1, 2$. The prior for $\boldsymbol{\theta}$ is defined through independent normal distributions for the α_j and the β_j, $j = 1, 2$. The choice of the prior parameters is discussed in the "Data Example" section below; the "Results" section addresses sensitivity of posterior inference to the prior specification.

Under this model formulation, Gibbs sampling (e.g., Robert and Casella 2004) is possible for all model parameters. Given the regime states, sampling the regime-specific parameters (α_j, β_j, V_j) requires only standard techniques for Bayesian regression problems (see, e.g., Gelman et al. 2004). Given the regime-specific parameters and adjacent regime states, sampling the regimes for each year involves only Bernoulli trials. Informally, the model fitting algorithm proceeds iteratively as follows.

1. Initialize by specifying starting values for parameters $\boldsymbol{\theta}$, $\boldsymbol{V}$ and $\boldsymbol{Q}$, and by assigning a regime state to each year.

2. Given the regime assignments, subdivide the data into regime-specific subsets and sample regime-specific parameter sets given this partition of the data. (This step updates parameters $\boldsymbol{\theta}$ and $\boldsymbol{V}$.)

3. Given the regime-specific parameters and regime states for each adjacent year, sample regime designations. (This step updates each regime state r_t, $t = 2, ..., T$.)

4. Given the regime states for all years, sample the transition probabilities. (This

step updates parameters q_{11} and q_{22} that define $\boldsymbol{Q}$.)

5. Repeat steps 2-4 many times.

Appendix A provides formal details on Gibbs sampling from the posterior of the model in Eq. 4. In the next section, we discuss how the posterior samples can be used for various types of inference that are of interest under our modeling framework.

Note that the standard Ricker model for the regime-specific recruitment relationships strikes a good balance between inferential flexibility and model parsimony for the Japanese sardine data considered in this paper. In general, we might seek more flexible specifications for the recruitment functions (e.g., the three-parameter Shepherd (1982) and Murray (2002) models) and/or the regime-specific distributions (e.g., heavier tailed or skewed distributions replacing the normals in Eq. 4). In principle, such model elaborations can be readily incorporated in the hierarchical modeling framework of Eq. 4. Moreover, semiparametric modeling can be proposed utilizing nonparametric priors for the regime-specific density dependence functions as in Munch et. al. (2005b). The methodology related with this latter extension will be reported elsewhere.

Posterior predicitive inference

There are a number of useful inferential quantities that emerge from the proposed modeling framework. First, estimates of the regime history, $\Pr(r_t = 1|\text{data})$, can be obtained directly from the posterior samples for the regime states for each year. This

posterior probability allows us, for instance, to determine how confident we are of the regime state for any year in the observed series.

We also obtain estimates of the long-run (stationary) distribution of recruitment, $p(y \mid S, \boldsymbol{Q}, \boldsymbol{\theta}, \boldsymbol{V})$. Although not applicable to any particular year, this distribution indicates the average probability of observing a given level of recuitment over a long period of time and may be useful in establishing sustainable harvest strategies.

Perhaps more useful in the short term is a prediction of next year's recruitment level, y_{T+1}, given the observed time series and next year's cohort size, S_{T+1}. This type of predictive inference can be obtained through the posterior forecast density, $p(y_{T+1} \mid S_{T+1}, \text{data})$, which takes into account the sequential dependence of the regime states when forecasting recruitment. When sequential dependence is high, this approach will provide recruitment predictions that are considerably more precise than would be possible with a single-regime model. When sequential dependence is less strong, the recruitment density is a mixture of log-normal distributions which allows the reasonable possibility that recruitment is bimodal.

Details on how these posterior predictive distributions are estimated are provided in Appendix B. Illustrations based on the Japanese sardine data are given in Figures 3 and 4.

Model comparison

The method we have proposed is intended explicitly for modeling recruitment when

there are multiple environmental regimes. However, in some situations it may be unclear whether there are distinct environmental regimes or whether there is a single, perhaps continuously varying, environmental state. Consequently, we need an approach to compare the proposed two-regime model in Eq. 4 to a model with only one regime. Under the single-regime model, we have $y_t \mid \boldsymbol{\theta}', V'$ independent $N(y_t \mid F(S_t; \boldsymbol{\theta}'), V')$, $t = 1, ..., T$, with $\boldsymbol{\theta}' = (\alpha', \beta')$ and the recruitment function given by $F(S; \boldsymbol{\theta}') = \alpha' - \beta' S$. We denote the single-regime and two-regime models by $\mathcal{M}_1$ and $\mathcal{M}_2$, respectively.

Although several approaches have been proposed for formal Bayesian model comparison, here we simply compare model performance using estimates for posterior probabilities, $\Pr(\mathcal{M}_1 \mid \text{data})$ and $\Pr(\mathcal{M}_2 \mid \text{data})$, associated with models $\mathcal{M}_1$ and $\mathcal{M}_2$. Importantly, these model probabilities are equivalent to posterior estimates for the number of regimes in a more general model that treats the number of regimes as random (with possible values 1 and 2). This method is customarily used in the context of Bayesian modeling with HMMs to estimate the number of hidden states (see, e.g., Scott, 2002, and further references therein). It therefore provides a natural approach to the model selection problem, since, in general, it can be extended to handle any finite number of regimes.

These posterior model probabilities are estimated using the posterior samples from the two models (as detailed in Appendix C). The approach requires specification of prior probabilities associated with the two models. As discussed in the "Results" section,

the application of the proposed methodology to the Japanese sardine data has revealed strong support for the two-regime model even under very small prior probabilities for this model.

DATA EXAMPLE

We consider application of the methodology to the analysis of recruitment data for Japanese sardine, previously studied by Wada and Jacobson (1998). Egg production estimates (S) were calculated from annual ichthyoplankton surveys (eggs/yr). The recruitment indices (R) are catch per unit effort data (tonnes per hour of search time) from a winter purse seine fishery and we assume, as did Wada and Jacobson, that these index abundance of age-0 recruits in December. We used data from 1977-1995 (reported in Wada and Jacobson 1998, Table 1, see our Figure 1 1).

Given the previously established regime shifts in Pacific species, we expect to be able to identify distinct regime-specific differences in survival to age 1. This is also consistent with previous analyses of the Japanese sardine data (see, e.g., the discussion in Wada and Jacobson, 1998). However, to our knowledge, this recruitment time series has not been studied within a modeling framework that simultaneously estimates probabilities of regime switching and parameters for the regime-specific recruitment relationships.

We fit the model in Eq 4. to these data, using a fairly noninformative prior specification for the transition probabilities and the regime-specific recruitment parameters. In particular, we used uniform priors for the q_{jj}, $j = 1, 2$, and identical independent

normal priors for each regime with mean log(4) for α_j, 0 for β_j, and large prior variance (equal to 10) for each of these parameters.

The error variances V_j were assigned more informative priors, specifically, (independent) inverse gamma distributions with prior expectation 0.5 and coefficient of variation (CV) 0.7, for $j = 1, 2$. The implications of this prior choice are reflected in the prior long-run density (Figure 3, top panel), which is estimated as discussed in Appendix B.

In the interest of model comparison, we also consider a single-regime Ricker model for these data. In this case, the normal priors for α' and β' were identical to those under the two-regime model. To allow for the greater variability in recruitment that must occur under a single-regime model, the error variance V' was given an inverse gamma prior with expectation 1 and CV 0.58. We obtained similar results using the same prior for V' that was used in the two-regime model.

RESULTS

We ran the Gibbs sampler described in Appendix A for 40000 iterations. We assessed convergence empirically using the Gelman-Rubin diagnostic (e.g., Gelman et al. 2004), which is based on between- and within-chain variances for each parameter, resulting from a number of parallel chains corresponding to different starting values for the Gibbs sampler. Although convergence was obtained within the first 500 samples, we used a conservative burn-in period of 10000 iterations. Autocorrelation within chains dropped below 0.05 in less than 30 samples for all parameters. Thus the 30000 samples

we retained represent approximately 1000 independent draws from the posterior.

The two-regime model fits the Japanese sardine data quite well. The posterior estimate of the long-run density (see Eq. 5 in Appendix B) shows clearly separated, recruitment regimes (Figure 3, bottom panel), and the inferred regime states (Figure 4, bottom panel) agree fairly well with the previously described environmental regimes.

Moreover, the two-regime model significantly outperformed a single-regime model. Based on estimated posterior model probabilities (see Appendix C for details), the data strongly support the existence of distinct recruitment regimes under practically any choice of prior probability, $\Pr(\mathcal{M}_2)$, for the two-regime model. For instance, the estimates for $\Pr(\mathcal{M}_2 \mid \text{data})$ were 0.936, 0.955, 0.977, and 0.991 under respective prior probabilities $\Pr(\mathcal{M}_2) = 0.1$, 0.2, 0.5, and 0.9. Even under the extreme choice $\Pr(\mathcal{M}_2) = 0.01$, we obtain an estimated posterior probability of 0.825 for the two-regime model. Thus, our results strongly support Wada and Jacobson's (1998) previous assertion that there are two recruitment regimes for Japanese sardines. Moreover, our regime estimates qualitatively agree with their division of the time series into a favorable regime from 1971-1987 and unfavorable regime from 1988-1995.

Posterior distributions for the model parameters (Figure 2) indicate substantial learning for most of the parameters; see also Table 1 as well as the prior and posterior estimates for the long-run density (Figure 3). The posterior distributions for the transition probabilities indicate some serial dependence in regime state (that is, both

q_{11} and q_{22} have most of their posterior probability mass at values greater than 0.5), though somewhat less than expected for regimes exhibiting decadal scale oscillations. Interestingly, there is a somewhat greater tendancy to remain in the low recruitment regime (e.g., $E(q_{22} \mid \text{data}) = 0.67$ and $E(q_{11} \mid \text{data}) = 0.58$). The posteriors for both of the density-dependence parameters were different across regimes. The maximum reproduction rate α was substantially lower and the effect of density β was substantially greater in the low recruitment regime. The posteriors for the error variances were also different in the two regimes, for instance, the posterior mean variability under the low recruitment regime was nearly twice of that in the high recruitment regime.

We conducted several sensitivity runs to evaluate the dependence of the results on the prior specification. Given the well documented decadal scale oscillations in many Pacific recruitment series, we might reasonably have asserted that the q_{jj} should be centered in their prior around, say, 0.9 resulting in one regime shift per decade, on average. We found that such more informative prior specifications for the q_{jj} made no qualitative difference to our results. The only quantitative differences were that the posterior regime classifications were less ambiguous for the most poorly classified years, i.e., years 1978, 1979, 1982, and 1992 (see Figure 4, bottom panel). Increasing the (already significant) prior uncertainty in the regression parameters α_j and β_j by a factor of 5 did not change the results. Finally, we found that increasing the prior uncertainty in the error variances V_j results in overdispersed, bimodal posteriors for

the α_j and β_j. This is a manifestation of the label switching issue that can arise in fitting mixture models (see the related discussion in Appendix A). Reducing the prior uncertainty for the V_j did not alter the results. Thus, under an inverse gamma specification for the prior, a CV of about 0.7 is as diffuse as possible while allowing clear identification of the recruitment regimes. Hence, in general, the error variances are the parameters that require the most careful prior elicitation in order to apply the two-regime model.

Interestingly, there were three years (1979, 1982, and 1992) in which the regime state differed from expectation based on prior analyses of environmental variables (Tian et al. 2004, Hare and Mantua 2000). These years were also among the most poorly classified. Analyses with alternative regresssion functions (Beverton-Holt or Shepherd) did not change this result indicating that the poor classification is not likely to stem from the assumed form for density dependence. Instead, we suspect that these years are poorly classified because they indicate exceptional recruitment for the expected regime. Removing the data for these years did not substantially alter inference for any of the regime-specific parameters, but did increase the probability of remaining in each regime (for instance, with data from years 1982 and 1992 removed, $E(q_{22} \mid \text{data}) = 0.83$ and $E(q_{11} \mid \text{data}) = 0.75$).

DISCUSSION

There are many attempts (on the order of hundreds) to incorporate environmental

variables into density dependence models for juvenile survival (e.g., Cushing 1982, Drinkwater and Myers 1987). In ideal situations, (e.g., Koster et al. 2001) a model incorporating physiologically relevant environmental variables can be constructed from a series of stage-specific observations. More typically, however, the approach used is to multiply a Ricker model by some additional function of the environment (e.g., Madenjian et al. 2005, Majormaki 2004, Kuikka et al. 1999).

Recent efforts indicate that aggregate variables such as the NAO index or PDO index are better predictors of ecological processes than more mechanistically interpretable variables such as temperature. Hallett et al. (2004) suggest that this result is driven by the complexity of the interactions between weather and ecology; because the specific environmental mechanisms that are most important in any year may vary, aggregate variables such as the NAO do a better job in coarse-grained analyses. Cianelli et al (2004, 2005) develop models for the survival of pre-recruitment stages of walleye pollock in the Gulf of Alaska using variations of generalized additive models (GAMs) to account for environmental factors. Their best model is a threshold GAM; in a particular region of the environmental variable space, log-survival is the sum of functions of population density and environmental variables (the standard multiplicative approach in a nonparametric context), but when a linear combination of the environmental variables exceeds a threshold a different set of nonparametric functions are applied to density and the environmental variables.

In a vein similar to our work, Peterman and colleagues (Peterman et al. 2000, 2003, Holt and Peterman 2004) have developed approaches in which environmental variables are incorporated implicitly. Peterman et al. (2000) model the parameter a in $R(S) = aSf(S)$ as a random walk, with $a(t+1) = a(t) + W(t)$, where $W(t)$ represents a random component due to the environment. They use a Kalman filter for estimation. Peterman et al. (2003) apply this method to a number of Bristol Bay sockeye salmon stocks; Holt and Peterman (2004) apply a similar model to time varying age-at-maturity of sockeye salmon. Brodziak et al. (2001) use a single productivity function $aSf(S)$ but allow the errors about the stock recruitment relationship to be correlated.

Thus, most of the existing approaches modify a to represent explicit or implicit environmental fluctuations in density independent factors. However, given that regime changes are characterized by substantial changes in the prey and predator fields, which may affect the intensity of competition for resources, it is plausible that the nature of density dependence changes as well. Our method allows both the density dependent and density independent terms to vary across each of the regime states.

This greater flexibility is not without costs, however. The model contains substantially more parameters and requires that we know something about reasonable ranges for the error variances *a priori*. We expect that the primary value of this approach will be in situations when there are good prior extrinsic reasons to suspect that two

regimes are present. Obviously, the model will tend to find two "regimes" whenever the data are substantially overdispersed or aggregated into clumps of high and low values. However, in this case the mixture framework used here may better reflect the complexity of the data than the unimodal densities commonly used to model recruitment residuals. Determining just how well-separated two recruitment regimes need to be for the model to identify them is an important area for future investigation.

Although many correlations between recruitment and the environment have been demonstrated, these are rarely used in management (Myers 1998). There are two good reasons for this. The first is that environmental correlations are notoriously unreliable; the vast majority have failed to stand the test of time (Myers 1998). However, even when environmental variables are reliable determinants of recruitment, in order to use them to make predictions of future recruitment success, we must be able to forecast each of the relevant environmental variables. With the approach described here, the information necessary to forecast future regime states is estimated as part of the model. This can be used to forecast future recruitments conditional on the most recent regime estimates (Figure 4, top panel). These recruitment forecasts may be different than the long-run probability of recruitment, particularly when there is strong serial dependence in the regime states.

When environmental regimes persist long enough, it is possible to consider regime-specific management practices (MacCall 2002). If, on the other hand, the regime state

oscillates with high frequency, the predicted recruitment distribution will be multimodal leading to multimodal estimates of management reference points. In our analysis of the Japanese sardine, the posterior expectations for the probability or remaining in each regime are not very high indicating an average residence time of 2-3 years (4-6 years if outliers were removed) and the conditional recruitment predictions are strongly bimodal. Recognizing this multimodality may be helpful in establishing precautionary targets under fluctuating environmental regimes.

Our broad objective here is to introduce another tool for modeling the productivity of populations when it seems that the relationship is regularly changing. To be sure, a wide variety of approaches can be brought to bear on the same problem. Here we have shown how Bayesian regression approaches, coupled with Hidden Markov Models for unknown or poorly observed environmental states, provide a powerful tool to study the productivity of populations under changing environmental regimes.

ACKNOWLEDGEMENTS

The authors thank Marc Mangel for suggesting the problem and for helpful discussions. This work was partially funded by the Center for Stock Assessment Research (a training program between the NMFS Santa Cruz Laboratory and University of California, Santa Cruz), by an Ecosystems Tools grant from the National Marine Fisheries Service, and by NSF grants DEB-0727312 (S. Munch) and DEB-0727543 (A. Kottas).

LITERATURE CITED

Brodziak, J.K.T., W.J. Overholtz, and P.J. Rago. 2001. Does spawning stock affect recruitment of New England groundfish? Canadian Journal of Fisheries and Aquatic Sciences **58**:306–318.

Ciannelli, L., K.S. Chan, K.M. Bailey, and N.C. Stenseth. 2004. Nonadditive effects of the environment on the survival of a large marine fish population. Ecology **85**:3418–3427.

Ciannelli, L., K.M. Bailey, K-S. Chan, A. Belgrano, and N.C. Stenseth. 2005. Climate changes causing phase transitions of walleye pollock (theragra chalcogramma) recruitment dynamics. Proceedings of the Royal Society of London B **272**:1735–1743.

Cushing, D.H. 1982. Climate and Fisheries. Academic Press. London.

Daskalov, G.M. 2003. Long-term changes in fish abundance and environmental indices in the Black Sea. Marine Ecology Progress Series **255**:259–270.

Drinkwater, K.F. and R.A.Myers. 1987. Testing predictions of marine fish and shellfish landings from environmental variables. Canadian Journal of Fisheries and Aquatic Sciences **44**:1568–1573.

Elliot, J.M. 1994. Quantitative Ecology and the Brown Trout. Oxford University

Press, Oxford.

Folke, C., S. Carpenter, B. Walker, M. Scheffer, T. Elmqvist, L. Gunderson, and C.S. Holling. 2004. Regime shifts, resilience, and biodiversity in ecosystem management. Annual Review of Ecology Evolution and Systematics **35**:557–581.

Gelman, A., Carlin, J.B., Stern, H.S. and Rubin, D.B. 2004. Bayesian Data Analysis, Second Edition. Chapman & Hall/CRC.

Hallett, T.B., T. Coulson, J.G. Pilkington, T.H. Clutton-Brock, J.M. Pemberton, and B.T. Grenfell. 2004. Why large-scale climate indices seem to predict ecological processes better than local weather. Nature **430**:71–75.

Hare, S.R. and N.J. Mantua. 2000. Empirical evidence for North Pacific regime shifts in 1977 and 1989. Progress in Oceanography **47**:103–145.

Holt, C.A., and R.M. Peterman. 2004. Long-term trends in age-specific recruitment of sockeye salmon (Oncorhynchus nerka) in a changing environment. Canadian Journal of Fisheries and Aquatic Sciences **61**:2455–2470.

Jacobson, L.D., and A.D. MacCall. 1995. Stock-recruitment models for Pacific sardine (Sardinops-sagax). Canadian Journal of Fisheries and Aquatic Sciences **52**:566–577.

Kell, L.T., and P.J. Bromley. 2004. Implications for current management advice for

North Sea plaice (Pleuronectes platessa): Part II. Increased biological realism in recruitment, growth, density-dependent sexual maturation and the impact of sexual dimorphism and fishery discards. Journal of Sea Research **51**:301–312.

Kjesbu, O.S., P.R. Witthames, P. Solemdal, and M.G. Walker. 1998. Temporal variations in the fecundity of Arcto-Norwegian cod (Gadus morhua) in response to natural changes in food and temperature. Journal of Sea Research **40**:303–321.

Koster, F.W., H.-H. Hinrichsen, M.A.St. John, D. Schnack, B. R. MacKenzie, J. Tomkiewicz, and M. Plikshs. 2001. Developing Baltic cod recruitment models. II. Incorporation of environmental variability and species interaction. Canadian Journal of Fisheries and Aquatic Sciences **58**:1534–1556.

Kuikka, S. M. Hilden, H. Gislason, S. Hansson, H. Sparholt, and O. Varis. 1999. Modeling environmentally driven uncertainties in Baltic cod (Gadus morhua) management by Bayesian influence diagrams. Canadian Journal of Fisheries and Aquatic Sciences **56**:629–641.

Liu, J.S., A.F. Neuwald, and C.E. Lawrence. 1999. Markovian structures in biological sequence alignments. Journal of the American Statistical Association **94**:1–15.

MacCall, A.D. 2002. Fishery-management and stock-rebuilding prospects under conditions of low-frequency environmental variability and species interactions. Bulletin of Marine Science **70**:613–628.

Madenjian, C.P., T.O. Hook, E.S. Rutherford, D.M. Mason, T.E. Croley II, E.B. Szalai, and J.R. Bence. 2005. Recruitment variability of alewives in Lake Michigan. Transactions of the American Fisheries Society **134**:218–230.

Majormaki, T.J. 2004. Analysis of the spawning stock-recruitment relationship of vendace (Coregonus albula) with evaluation of alternative models, additional variables, biases, and errors. Ecology of Freshwater Fish **13**:46–60.

McFarlane, G.A., J.R.King, R.J. Beamish. 2000. Have there been recent changes in climate? Ask the fish. Progress in Oceanography **47**:147–169.

Mueter, F.J., J.L. Boldt, B.A. Megrey, and R.M. Peterman. 2007. Recruitment and survival of Northeast Pacific Ocean fish stocks: temporal trends, covariation, and regime shifts. Canadian Journal of Fisheries and Aquatic Sciences **64**: 911–927.

Munch, S.B., M.L. Snover, G.M. Watters, and M. Mangel. 2005a. A unified treatment of top-down and bottom-up control of reproduction in populations. Ecology Letters **8**:691–695.

Munch, S.B., A. Kottas, and M. Mangel. 2005b. Bayesian nonparametric analysis of stock-recruitment relationships. Canadian Journal of Fisheries and Aquatic Sciences **62**:1808–1821.

Murray, J.D. 2002. Mathematical Biology I: An Introduction. Springer Verlag, New York.

Myers, R.A. 1998. When do environment-recruitment correlations work? Reviews in Fish Biology and Fisheries. 8:285-305.

Nisbet, R.M., and J.R. Bence. 1989. Alternative Dynamics Regimes for Canopy-Forming Kelp: A Variant on Density-Vague Population Regulation. The American Naturalist **134**:377–408.

Peterman, R.M., B.J. Pyper, and J.A. Grout. 2000. Comparison of parameter estimation methods for detecting climate-induced changes in productivity of Pacific salmon (Oncorhynchus spp.). Canadian Journal of Fisheries and Aquatic Sciences **57**:181–191.

Peterman, R.M., B.J. Pyper, and B.W. MacGregor. 2003. Use of the Kalman filter to reconstruct historical trends in productivity of Bristol Bay sockeye salmon (Oncorhynchus nerka). Canadian Journal of Fisheries and Aquatic Sciences **60**:809–824.

Ricker, W.E. 1954. Stock and recruitment. Journal of the Fisheries Research Board of Canada **11**:559-623.

Robert, C.P., and G. Casella. 2004. Monte Carlo Statistical Methods, Second Edition. Springer, New York.

Scheffer, M., and S. Carpenter. 2003. Catastrophic regime shifts in ecosystems: linking theory to observation. TRENDS in Ecology and Evolution **18**:648–656.

Scheffer, M., S. Carpenter, J.A. Foley, C. Folke, and B. Walker. 2001. Catastrophic shfits in ecosystems. Nature **413**:591–596.

Scott, S.L. 2002. Bayesian methods for hidden Markov models: Recursive computing in the 21st century. Journal of the American Statistical Association **97**:337–351.

Shepherd, J.G. 1982. A versatile new stock-recruitment relationship for fisheries and the construction of sustainable yield curves. Journal du Conseil **40**:67–75.

Slatkin, M. 1978. Dynamics of a Population in a Markovian Environment. Ecology **59**:249–256.

Sugimoto, T. S. Kimua, and K. Tadokoro. 2001. Impact of El Nino events and climate regime shift on living resources in the western North Pacific. Progress in Oceanography **49**:113–127.

Tian, Y., Y. Ueno, M. Suda, and T. Akamine. 2004. Decadal variability in the abundance of Pacific saury and its response to climatic/oceanic regime shifts in the northwestern subtropical Pacific during the last half-century. Journal of Marine Systems **52**:235–257.

Tucker, B.C., and M. Anand. 2004. The Application of Markov models in Recovery and Restoration. International Journal of Ecology and Environmental Sciences **30**:131–140.

Wada, T., and L.D. Jacobson. 1998. Regimes and stock-recruitment relationships in Japanese sardine (Sardinops melanostictus), 1951-1995. Canadian Journal of Fisheries and Aquatic Sciences **55**:2455–2463.

Welch, D.W., B.R. Ward, B.D. Smith, J.P. Eveson 2000. Temporal and spatial responses of British Columbia steelhead (Oncorhynchus mykiss) populations to ocean climate shifts. Fisheries Oceanography **9**:17–32.

APPENDIX A. Computational approach to sampling the posterior

Here, we describe the details of the algorithm used to obtain samples from the posterior of the model in Eq. 4.

Let data $= \{(y_t, S_t) : t = 1, ..., T\}$ be the set of observations and denote by $p(\boldsymbol{\theta}, \boldsymbol{V}, \boldsymbol{Q}, \boldsymbol{r} \mid \text{data})$ the posterior for all parameters, including the regime states $\boldsymbol{r} = (r_2, ..., r_T)$. Sampling from this posterior was accomplished with standard posterior simulation methods for HMMs (see, e.g., Scott 2002 and references therein). In particular, as discussed briefly in the "Methods" section, we used Gibbs sampling cycling over posterior full conditional distributions as detailed below.

For each $t = 2, ..., T-1$, the full conditional posterior probability that the regime is in state 1 in year t, i.e., $\Pr(r_t = 1 \mid \boldsymbol{\theta}, \boldsymbol{Q}, \boldsymbol{V}, \boldsymbol{r}_{-t}, \text{data})$, is given by

$$\frac{N(y_t \mid F(S_t; \boldsymbol{\theta}_1), V_1)\Pr(r_t = 1 \mid r_{t-1}, \boldsymbol{Q})\Pr(r_{t+1} \mid r_t = 1, \boldsymbol{Q})}{\sum_{j=1}^{2} N(y_t \mid F(S_t; \boldsymbol{\theta}_j), V_j)\Pr(r_t = j \mid r_{t-1}, \boldsymbol{Q})\Pr(r_{t+1} \mid r_t = j, \boldsymbol{Q})}$$

where $\boldsymbol{r}_{-t}$ indicates the set of regime states with r_t removed. The corresponding posterior probability for r_T is

$$\Pr(r_T = 1 \mid \boldsymbol{\theta}, \boldsymbol{Q}, \boldsymbol{V}, r_{T-1}, \text{data}) = \frac{N(y_T \mid F(S_T; \boldsymbol{\theta}_1), V_1)\Pr(r_T = 1 \mid r_{T-1}, \boldsymbol{Q})}{\sum_{j=1}^{2} N(y_T \mid F(S_T; \boldsymbol{\theta}_j), V_j)\Pr(r_T = j \mid r_{T-1}, \boldsymbol{Q})}.$$

The full conditionals for the transition probabilities are given by Beta distributions with parameters determined by the corresponding priors, and the number n_{kl} of transitions into state l from state k based on the current sample of regime states $\boldsymbol{r}$. We

denote by v_j and w_j the parameters of the Beta priors for each q_{jj}, $j = 1, 2$. Then, the posterior full conditional for q_{11} is given by a Beta distribution with parameters $n_{11} + v_1$ and $n_{12} + w_1$. Analogously, the posterior full conditional for q_{22} is a Beta distribution with parameters $n_{22} + v_2$ and $n_{21} + w_2$.

The full conditionals for the error variances are given by inverse gamma distributions with parameters determined by the priors and regime-specific residual sum-of-squares. Denote by A_{V_j} the shape parameter and by B_{V_j} the scale parameter of the inverse gamma prior for the error variance V_j (we use the parameterization of the inverse gamma that yields prior mean $B_{V_j}/(A_{V_j} - 1)$, provided $A_{V_j} > 1$). Then, for each $j = 1, 2$, the posterior full conditional for V_j is an inverse gamma distribution with scale parameter $B_{V_j} + 0.5 \sum_{\{t:r_t=j\}} \{y_t - F(S_t; \boldsymbol{\theta}_j)\}^2$ and shape parameter $A_{V_j} + 0.5T_j$, where T_j is the total number of years t for which $r_t = j$.

The full conditionals for the regime-specific regression parameters are bivariate normal. Let A_{α_j}, A_{β_j} and B_{α_j}, B_{β_j} be the means and variances, respectively, of the normal prior distributions for the α_j and β_j. Then, for each $j = 1, 2$, the posterior full conditional for (α_j, β_j) is given, up to the normalizing constant, by

$$p(\alpha_j)p(\beta_j) \prod_{\{t:r_t=j\}} N(y_t \mid \alpha_j - \beta_j S_t, V_j),$$

where $p(\alpha_j)$ and $p(\beta_j)$ are the prior densities for α_j and β_j, respectively. Note that the product above can be written in the form of a T_j-dimensional normal distribution for $\boldsymbol{y}_j = \{y_t : r_t = j\}$ with mean vector $\boldsymbol{S}_j(\alpha_j, \beta_j)^{\mathrm{T}}$ and covariance ma-

trix $V_j\boldsymbol{I}$. Here, superscript T denotes transpose operations, $\boldsymbol{I}$ is the $T_j \times T_j$ identity matrix, and $\boldsymbol{S}_j$ is the $T_j \times 2$ matrix with all first column elements equal to 1 and second column given by the T_j-dimensional vector $\{-S_t : r_t = j\}$. Hence, using standard Bayesian updating calculations for normal linear regression models, the posterior full conditional for (α_j, β_j) can be shown to be bivariate normal with covariance matrix $\Sigma_{\alpha,\beta} = (\text{diag}(B_{\alpha_j}^{-1}, B_{\beta_j}^{-1}) + V_j^{-1}\boldsymbol{S}_j^{\mathrm{T}}\boldsymbol{S}_j)^{-1}$ and mean vector $\boldsymbol{\mu}_{\alpha,\beta} = \Sigma_{\alpha,\beta}((A_{\alpha_j}B_{\alpha_j}^{-1}, A_{\beta_j}B_{\beta_j}^{-1})^{\mathrm{T}} + V_j^{-1}\boldsymbol{S}_j^{\mathrm{T}}\boldsymbol{y}_j)$.

We note that the model structure is, in principle, unidentifiable. Since the regime designation is arbitrary, for any data set there are two equally probable solutions corresponding to swapping the regime labels. That is, under one solution, some set of observations are assigned to group 1, the remainder to group 2 and parameters for each group are determined appropriately. The other equally reasonable solution is to swap group assignments for all members of each group and update parameter distributions accordingly. Thus, for sufficiently close regime-specific parameter sets, the algorithm will switch regime assignments for all (or nearly all) observations between each jump resulting in bimodal posteriors for the parameters and equiprobable group assignment. The regime-specific regression parameters for the sardine data were sufficiently well separated that label switching was not a problem under the carefully chosen, but arguably reasonable, prior for the regime-specific error variances (discussed in the "Results" section). In other cases, the label switching problem may be dealt with by

incorporating additional structure into the priors for the regression parameters or by incorporating an additional acceptance criterion into the Gibbs sampler that preserves regime identity. For instance, one possibility would be to restrict one regime to have higher recruitment at some specified stock size; alternatively, the priors for the α_j can be constrained to support a monotonicity restriction with larger values corresponding to the high regime.

APPENDIX B. Posterior predictive inference

We describe here how posterior inference can be obtained for the hidden regime states and the long-run recruitment distribution. We also show how the posterior predictive distribution for the next year's recruitment is obtained.

The Gibbs sampler developed in Appendix A yields B posterior samples $\{r_{t,b} : b = 1, ..., B\}$ for each regime state r_t (as well as for all other parameters of the model in Eq. 4). These samples were tallied to estimate, for each year, the posterior probability of being in regime 1, $\Pr(r_t = 1|\text{data})$. For instance, $B^{-1} \sum_{b=1}^{B} I_{(r_{t,b}=1)}$ is a natural estimate for $\Pr(r_t = 1|\text{data})$, where $I_{(r_{t,b}=1)}$ is equal to 1 if $r_{t,b} = 1$ and is equal to 0 otherwise. Figure 4 (bottom panel) shows these estimates for the Japanese sardine recruitment data.

The long-run marginal density of recruitment, y, for any particular initial cohort

size, S, can also be obtained from the posterior samples. This density is given by

$$p(y \mid S, \boldsymbol{Q}, \boldsymbol{\theta}, \boldsymbol{V}) = \pi N(y \mid F(S; \boldsymbol{\theta}_1), V_1) + (1 - \pi) N(y \mid F(S; \boldsymbol{\theta}_2), V_2), \tag{5}$$

where π is the stationary (long-run) probability of regime 1, which is defined through the transition probabilities in $\boldsymbol{Q}$, specifically, $\pi = (1 - q_{22})/(2 - q_{11} - q_{22})$. Hence, for each pair of values (S, y) over an appropriate grid, the posterior long-run density $p(y \mid S, \boldsymbol{Q}, \boldsymbol{\theta}, \boldsymbol{V})$ is estimated by averaging the expression on the right hand side of Eq. 5 over the posterior samples for $\boldsymbol{\theta}$, $\boldsymbol{V}$ and π, the latter emerging directly from the posterior samples for $\boldsymbol{Q}$.

Note that the long-run density provides also a useful means of studying prior-to-posterior learning. In particular, the implications of the prior choice for parameters $\boldsymbol{Q}$, $\boldsymbol{\theta}$ and $\boldsymbol{V}$ can be studied working with the corresponding long-run density. The prior long-run density can be estimated using, again, the expression in Eq. 5, which is now averaged over the prior distributions (or samples from the prior distributions) for $\boldsymbol{\theta}$, $\boldsymbol{V}$ and π, where the prior distribution for π is induced by the prior for $\boldsymbol{Q}$. Figure 3 plots prior and posterior estimates for the long-run density of recruitment for Japanese sardines.

Perhaps more useful than the long-run recruitment density is the posterior forecast density of the next year's recruitment, y_{T+1}, for a given cohort size, S_{T+1}. We denote this posterior forecast density by $p(y_{T+1} \mid S_{T+1}, \text{data})$. This is distinct from the long-run density of recruitment in that it explicitly takes into account the dependence of

next year's regime state, r_{T+1}, on the regime state in year T. The posterior forecast density is defined by averaging over the posterior $p(\boldsymbol{\theta}, \boldsymbol{V}, \boldsymbol{Q}, \boldsymbol{r} \mid \text{data})$ the following conditional density,

$$p(y_{T+1} \mid S_{T+1}, r_T, \boldsymbol{\theta}, \boldsymbol{V}, \boldsymbol{Q}) = \sum_{j=1}^{2} \Pr(r_{T+1} = j | r_T, \boldsymbol{Q}) N(y_{T+1} \mid F(S_{T+1}; \boldsymbol{\theta}_j), V_j).$$

It can thus be readily estimated using the samples from $p(\boldsymbol{\theta}, \boldsymbol{V}, \boldsymbol{Q}, \boldsymbol{r} \mid \text{data})$. An illustration, based on the sardine data, is given in the top panel of Figure 4.

APPENDIX C. Estimation of posterior model probabilities

Here, we discuss computing for the posterior probabilities corresponding to the Ricker model and the two-regime model. As discussed in the "Model comparison" section, the approach is to consider the general model that incorporates uncertainty regarding the number of regimes, which is therefore now a random variable (denoted here by k) with possible values 1 and 2. Hence, $k = 1$ corresponds to the single-regime Ricker model (model $\mathcal{M}_1$) and $k = 2$ to the two-component switching regression model in Eq. 4 (model $\mathcal{M}_2$). We develop an estimate for $\Pr(\mathcal{M}_2 \mid \text{data}) \equiv \Pr(k = 2 \mid \text{data})$ (where $\Pr(k = 1 \mid \text{data}) = 1 - \Pr(k = 2 \mid \text{data})$).

Let $\boldsymbol{\phi}_1 = (\alpha', \beta', V')$ and $\boldsymbol{\phi}_2 = (\boldsymbol{\theta}, \boldsymbol{V}, \boldsymbol{Q})$ denote the parameters of the Ricker and two-regime models, respectively. Assume that the joint prior is built from independent components for $\boldsymbol{\phi}_1$, $\boldsymbol{\phi}_2$ and k, the latter requiring $\Pr(\mathcal{M}_2) \equiv \Pr(k = 2)$ (with $\Pr(k = 1) = 1 - \Pr(k = 2)$). Then, given k, $\boldsymbol{\phi}_1$ and $\boldsymbol{\phi}_2$ are conditionally independent in

their posterior distribution. Hence, $p(\boldsymbol{\phi}_1, \boldsymbol{\phi}_2 \mid \text{data})$ can be obtained using two parallel Gibbs samplers, the one described in Appendix A for model $\mathcal{M}_2$, and a standard Gibbs sampler for normal linear regression for model $\mathcal{M}_1$. Moreover, $\Pr(k = 2 \mid \text{data}) = \int \Pr(k = 2 \mid \boldsymbol{\phi}_1, \boldsymbol{\phi}_2, \text{data}) p(\boldsymbol{\phi}_1, \boldsymbol{\phi}_2 \mid \text{data}) \mathrm{d}\boldsymbol{\phi}_1 \mathrm{d}\boldsymbol{\phi}_2$, where

$$\Pr(k = 2 \mid \boldsymbol{\phi}_1, \boldsymbol{\phi}_2, \text{data}) = \frac{p(\text{data} \mid \boldsymbol{\phi}_2, k = 2)\Pr(k = 2)}{p(\text{data} \mid \boldsymbol{\phi}_1, k = 1)\Pr(k = 1) + p(\text{data} \mid \boldsymbol{\phi}_2, k = 2)\Pr(k = 2)}.$$

Here, $p(\text{data} \mid \boldsymbol{\phi}_\ell, k = \ell)$ is the likelihood under model $\mathcal{M}_\ell$, $\ell = 1, 2$. Therefore, the estimate for $\Pr(k = 2 \mid \text{data})$ can be obtained by Monte Carlo integration of its expression using the posterior samples for $\boldsymbol{\phi}_1$ and $\boldsymbol{\phi}_2$.

The estimate requires evaluation of the model likelihoods $p(\text{data} \mid \boldsymbol{\phi}_\ell, k = \ell)$, $\ell = 1, 2$, for each posterior sample. The likelihood under model $\mathcal{M}_1$ is easy to compute directly. However, the two-regime model likelihood is given by

$$p(\text{data} \mid \boldsymbol{\phi}_2, k = 2) = \sum N(y_1 \mid \alpha_1 - \beta_1 S_1, V_1) \prod_{t=2}^{T} \Pr(r_t \mid r_{t-1}) N(y_t \mid \alpha_{r_t} - \beta_{r_t} S_t, V_{r_t})$$

where the sum is over all possible configurations of the vector $\boldsymbol{r} = (r_2, ..., r_T)$. Direct evaluation of this likelihood requires $O(2^{T-1})$ steps and is thus too expensive even for moderate T. The numbers of steps is reduced to $O(4(T-1))$ using the likelihood recursion, a standard computational method for HMMs (see, e.g., Scott, 2002). For $t = 1, ..., T$, let $\boldsymbol{d}^t$ be the vector that collects the data up to time point t (and thus data $= \boldsymbol{d}^T$). Moreover, for $t = 2, ..., T$, and $j = 1, 2$, define the "forward" variable $L_t(j) = p(\boldsymbol{d}^t, r_t = j \mid \boldsymbol{\phi}_2)$, that is, the joint likelihood contribution of $\boldsymbol{d}^t$ and event

$\{r_t = j\}$ (with $(r_2, ..., r_{t-1})$ marginalized). Note that the likelihood contribution from $\boldsymbol{d}^t$ is $L_t(1) + L_t(2)$, and thus $p(\text{data} \mid \boldsymbol{\phi}_2, k = 2) = L_T(1) + L_T(2)$. Because we set $r_1 = 1$, we have $L_1(1) = N(y_1 \mid \alpha_1 - \beta_1 S_1, V_1)$ and $L_1(2) = 0$. The likelihood recursion yields $\{L_t(j) : j = 1, 2\}$ from $\{L_{t-1}(j) : j = 1, 2\}$. In particular, for $t = 2, ..., T$ and $j = 1, 2$, it can be shown that $L_t(j) = N(y_t \mid \alpha_j - \beta_j S_t, V_j)\{q_{j1} L_{t-1}(1) + q_{j2} L_{t-1}(2)\}$. Therefore, this approach provides an efficient method of computing the two-regime model likelihood.

Table 1: Posterior summaries for the parameters of the two-regime model applied to the Japanese sardine data.

Posterior summary	α_1	β_1	α_2	β_2	V_1	V_2	q_{11}	q_{22}
Mean	-2.565	0.292	-4.124	0.735	0.378	0.656	0.580	0.673
SD	0.364	0.197	0.463	0.162	0.240	0.332	0.170	0.156
2.5th percentile	-3.427	0.084	-4.926	0.519	0.146	0.267	0.240	0.344
Median	-2.570	0.266	-4.167	0.742	0.311	0.572	0.587	0.683
97.5th percentile	-1.706	0.498	-3.054	0.972	1.033	1.544	0.892	0.937

Table 2: Posterior summaries for the parameters of a Ricker model fitted to the Japanese sardine data.

Posterior summary	α'	β'	V'
Mean	-3.414	0.502	2.184
SD	0.488	0.153	0.637
2.5th percentile	-4.350	0.203	1.259
Median	-3.424	0.503	2.078
97.5th percentile	-2.429	0.807	3.703

FIGURE LEGENDS

Figure 1: Plot of the Japanese sardines data on their original scale. The numbers indicate year for the observed data with lines connecting consecutive years.

Figure 2: Posteriors for model parameters under the two-regime model in Eq. 4 (denoted by the solid lines). The dashed line in each panel indicates the corresponding prior density.

Figure 3: The top panel shows the prior long-run density and the bottom panel plots the corresponding posterior long-run density (see Appendix B). The data are also included in the bottom panel (numbers indicate year with dashed lines connecting consecutive years). In both panels, the tone indicates the long-run density value with black being zero and lighter tone corresponding to higher density.

Figure 4: The top panel plots the posterior forecast density for next year's recruitment as a function of initial population size, including also the data (numbers indicate year with dashed lines connecting consecutive years). The tone indicates the value of the posterior forecast density with black being zero and lighter tone corresponding to higher density. The bottom panel shows posterior estimates (denoted by the black bars) for the probability of being in the high recruitment regime for each year.

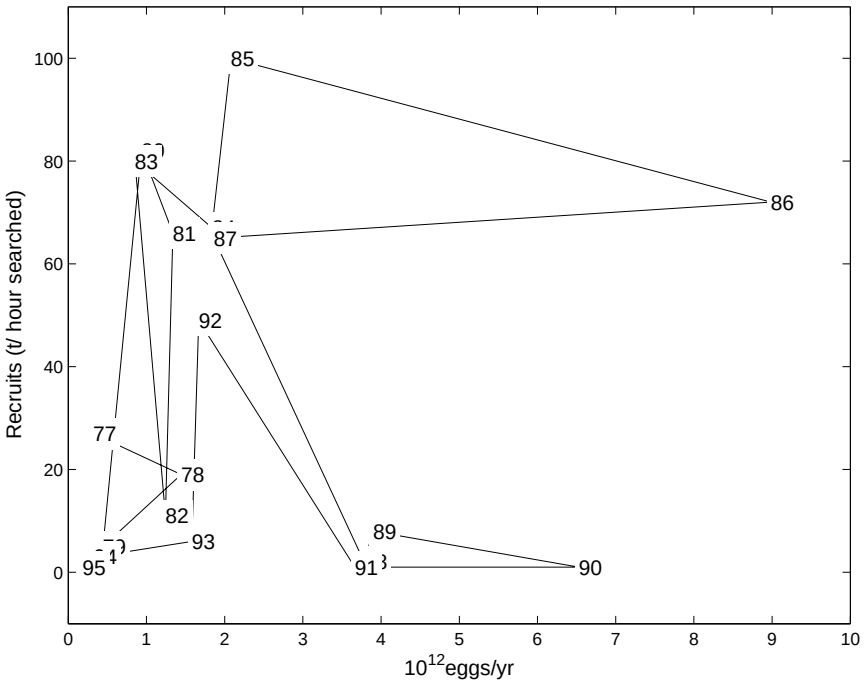
Recruits (t/ hour searched)
10^{12}eggs/yr
0
20
40
60
80
100
0
1
2
3
4
5
6
7
8
9
10
85
86
87
83
81
92
77
78
82
89
90
91
93
95

Figure 1:

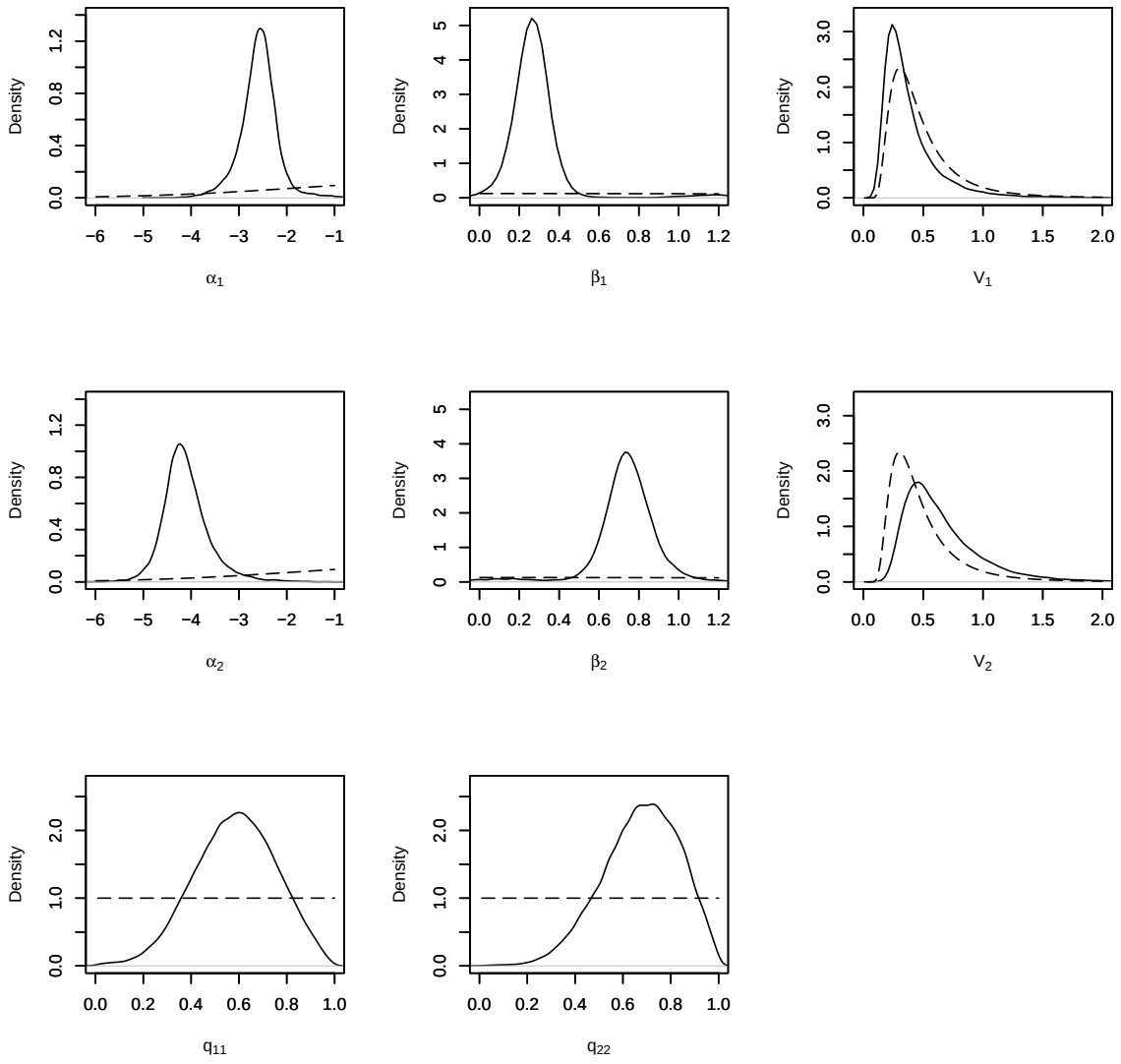

Figure 2:

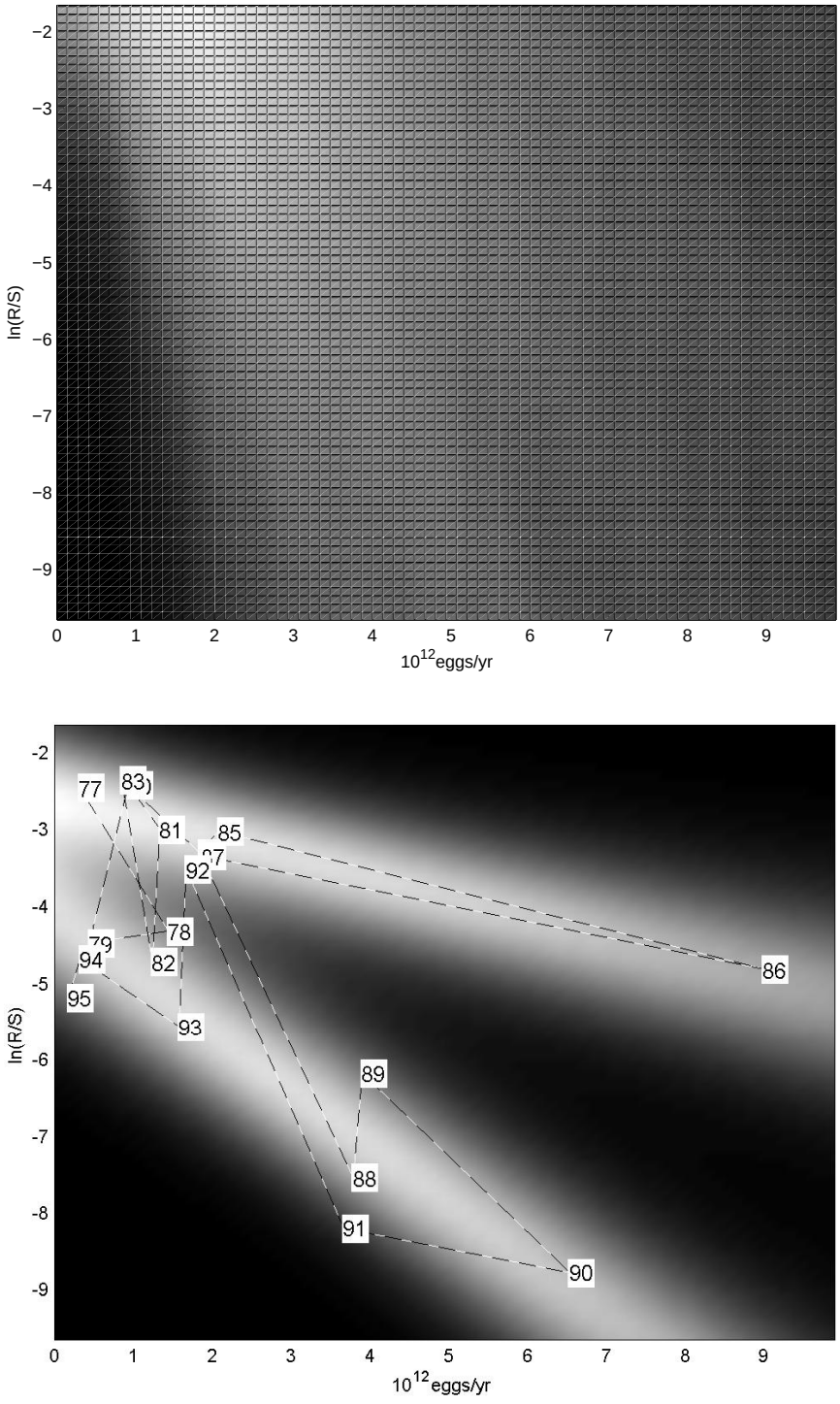
ln(R/S)
−2
−3
−4
−5
−6
−7
−8
−9
0
1
2
3
4
5
6
7
8
9
10^12eggs/yr
ln(R/S)
-2
-3
-4
-5
-6
-7
-8
-9
77
83
81
85
92
78
79
94
82
95
93
89
88
91
90
86
0
1
2
3
4
5
6
7
8
9
10^12eggs/yr

Figure 3:

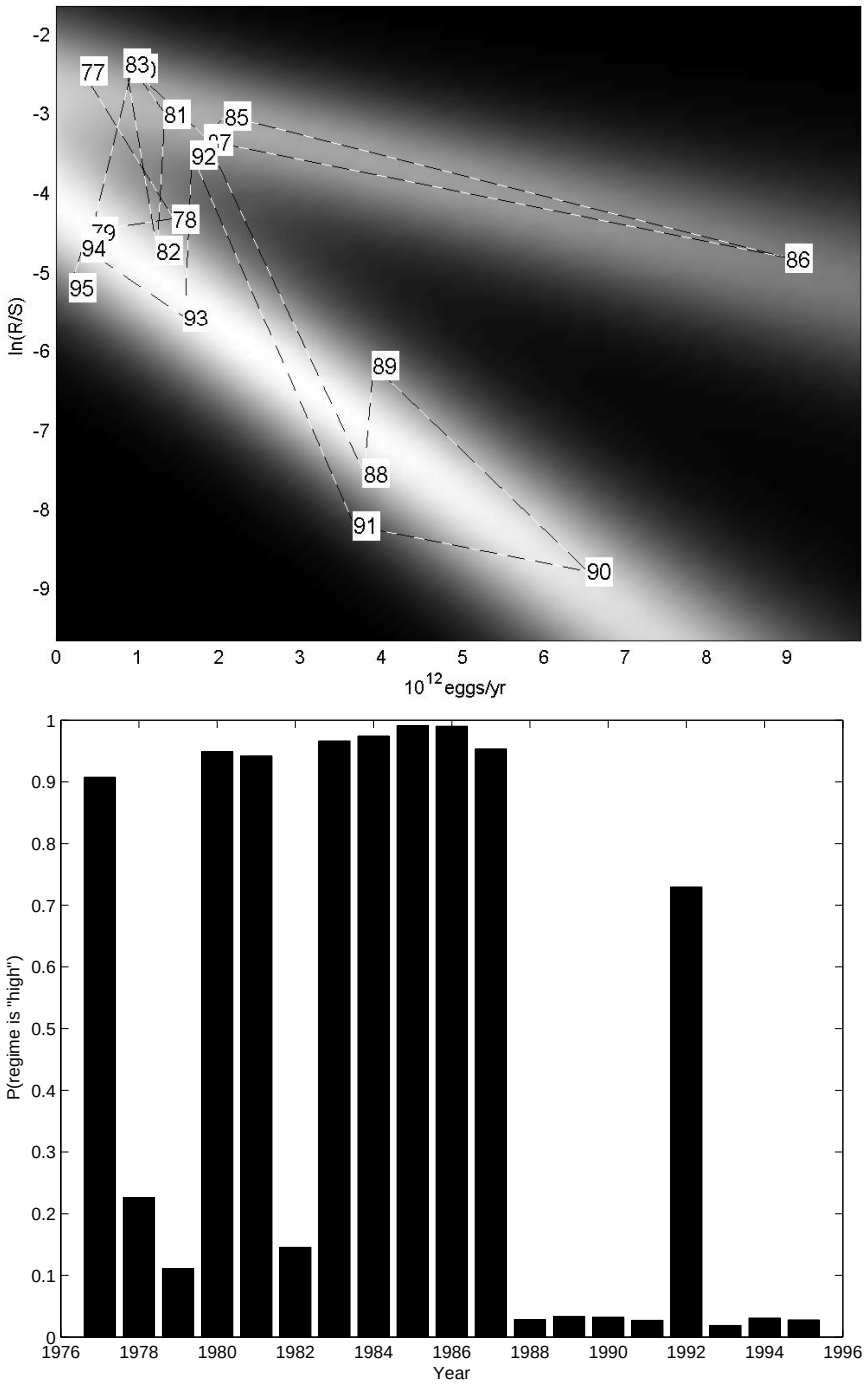
ln(R/S)
10^{12}eggs/yr
77
83
81
85
92
78
79
94
82
86
95
93
89
88
91
90
P(regime is "high")
Year

Figure 4: